Langmuir

Research Article

Structure of the Langmuir Monolayers with Fluorinated Ethyl Amide and Ethyl Ester Polar Heads Creating Dipole Potentials of Opposite Sign

Tonya D. Andreeva, Jordan G. Petrov, Gerald Brezesinski, and Helmuth Moehwald

Langmuir, **2008**, 24 (15), 8001-8007 • DOI: 10.1021/la8009282 • Publication Date (Web): 04 July 2008

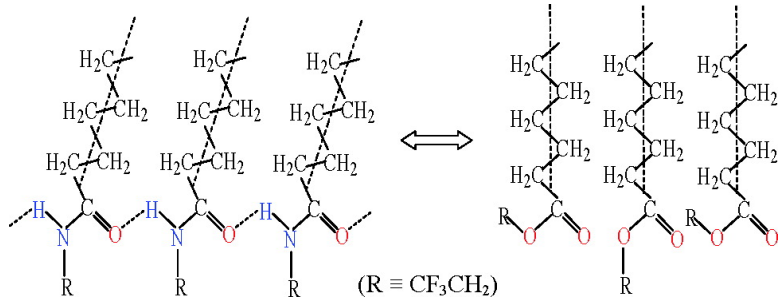

More About This Article

Additional resources and features associated with this article are available within the HTML version:

- Supporting Information
- Access to high resolution figures
- Links to articles and content related to this article
- Copyright permission to reproduce figures and/or text from this article

View the Full Text HTML

Structure of the Langmuir Monolayers with Fluorinated Ethyl Amide and Ethyl Ester Polar Heads Creating Dipole Potentials of Opposite Sign

Tonya D. Andreeva, Jordan G. Petrov,* Gerald Brezesinski, and Helmuth Moehwald

Max-Planck Institute of Colloids and Interfaces, D-14476 Golm/Potsdam, Germany

Received March 25, 2008. Revised Manuscript Received May 8, 2008

This study experimentally checks our previous hypothesis (Petrov, J. G.; Polymeropoulos, E. E.; Moehwald, H. *Langmuir* **2007**, *23*, 2623) that different conformations of the fluorinated heads of $RCONHCH_2CF_3$ and $RCOOCH_2CF_3$ monolayers cause the opposite signs and the striking difference of 1.480 V between their surface potentials ΔV. In situ X-ray diffraction at grazing incidence (GIXD) shows that both monolayers form orthorhombic lattices with closely packed chains tilted to the next-nearest neighbors in the $RCONHCH_2CF_3$ film and upright in the $RCOOCH_2CF_3$ monolayer. The packing of the chains in the plane perpendicular to them, which excludes the effect of the tilt, shows the same distance between the next-nearest neighbors, but significantly closer nearest neighbors in the $RCONHCH_2CF_3$ film. This difference implies a specific anisotropic attraction between the adjacent amide heads. IR reflection absorption spectroscopy (IRRAS) shows that the $-CONHCH_2CF_3$ heads have trans conformation and participate in H-bonds forming a $-NH\cdots O{=}C-$ lateral network. We speculate that such structure hinders the energetically optimal orientation of the hydrophobic $-CH_2CF_3$ terminals toward air, so that the $^{\delta+}C-(F^{\delta-})_3$ dipoles at the monolayer/water boundary yield a strong positive contribution to ΔV. In contrast, most of the unbounded by H-bonds $-COOCH_2CF_3$ heads statistically orient their hydrophobic $^{\delta+}C-(F^{\delta-})_3$ dipoles toward air, yielding a negative average dipole moment at the monolayer/water boundary and negative surface dipole potential.

Introduction

The dipole potential at the boundary biomembrane−aqueous environment regulates the binding energy and translocation rate of hydrophobic ions and ion-carriers, absorption and penetration of amphiphilic peptides and proteins, polarization of interfacial water, and membrane adhesion. We have shown[1−3] that designed amphiphilic molecules with fluorinated polar heads can reverse the sign or dramatically increase the positive value of the surface dipole potential ΔV of Langmuir monolayer model membranes. Monolayers with trifluoroethyl ester heads show negative dipole potentials shifted by 200% from the positive ΔV values of the nonfluorinated films,[1] whereas the *N*-trifluoroethyl amide heads increase by 300% the positive surface dipole potential of the nonfluorinated *N*-ethyl amide monolayers.[3] We hypothesized[3] that the striking difference of 1.48 V between the ΔV values of the $RCOOCH_2CF_3$ and $RCONHCH_2CF_3$ monolayers, having the same $C_{21}H_{43}$ hydrocarbon chains and very similar polar heads, results from different conformations that the amide and ester heads adopt in the monolayers. Such conformational dissimilarity could demonstrate itself in different molecular organization of the monolayers. Significant difference was found[4] between the morphology and the monolayer lattice structure of Langmuir films of glycerol amide and glycerol ester lipids that also differ only by the −HN− versus −O− groups linking the chain and the head. Here, we check the existence of structural difference between the $RCOOCH_2CF_3$ and $RCONHCH_2CF_3$ monolayers that could be related to their different electrostatic properties. In situ X-ray diffraction at grazing incidence (GIXD) and IR reflection absorption spectroscopy (IRRAS) were applied to study the $RCONHCH_2CF_3$ film, and the obtained results were compared with our previous GIXD data for the $RCOOCH_2CF_3$ monolayer[5] and literature IRRAS data for long chain esters.[6]

Experimental Section

Materials and Formation of the Monolayers. $CH_3(CH_2)_{20}CONHCH_2CF_3$ (FEA) and $CH_3(CH_2)_{20}COOCH_2CF_3$ (FEE) were synthesized at the Max-Planck Institute of Colloids and Interfaces by Dr. R. Wagner and Mrs. Y. Wu as described elsewhere.[1] Both substances were spread as 1×10^{-3} M chloroform solutions on Millipore Milli-Q water in the Teflon trough of a Langmuir balance with Wilhelmy dynamometric system. After 5 min passed for evaporation of the chloroform, the monolayers were compressed at a rate of 2.2 Å^2/molecule·min to the desired surface pressure, which was automatically maintained during the GIXD and IRRAS measurements. The aqueous substrate was kept at 20.0 ± 0.1 °C by a temperature control system.

GIXD Measurements. The structure of the monolayers was studied on a liquid surface diffractometer at the undulator beam line BW1, at HASYLAB, DESY in Hamburg, Germany, as described previously.[5] The repeat distances of the monolayer lattice $d_{hk} = 2\pi/Q_{xy}^{hk}$ calculated from the maximal horizontal (in-plane) components of the diffraction vector Q_{xy}^{hk} for different Miller indices h,k yield the primitive unit cell parameters a, b, c, α, β, γ and the area occupied by a molecule on the water surface $A_{xy} = ab \sin \gamma$. If the vertical (out-of-plane) component of the diffraction vector Q_z^{hk} is also registered, the tilt angle τ of the hydrocarbon chains from the surface normal can be calculated from the Q_{xy}^{hk} and Q_z^{hk} maxima of the peaks. When the monolayer has an orthorhombic lattice, one nondegenerate Q^n peak and one 2-fold degenerate Q^d peak appear in the diffractogram. For upright chains $Q_z^n = Q_z^d = 0$, a NN tilt (to next-neighbors) gives $Q_z^n = 0$ and $Q_z^d > 0$, and a NNN tilt (to

* Corresponding author. Permanent address: Institute of Biophysics, Bulgarian Academy of Sciences, 1 Acad. G. Bonchev Str., Block 21,1113 Sofia, Bulgaria. E-mail:jordangpetrov@yahoo.com.

(1) Petrov, J. G.; Möhwald, H. *J. Phys. Chem. B* **1996**, *100*, 18458.
(2) Petrov, J. G.; Andreeva, T. D.; Kurth, D. G.; Möhwald, H. *J. Phys. Chem. B* **2005**, *109*, 14102.
(3) Petrov, J. G.; Polymeropoulos, E. E.; Möhwald, H. *Langmuir* **2007**, *23*, 2623.
(4) Gehlert, U.; Weidemann, G.; Vollhardt, D.; Brezesinski, G.; Wagner, R.; Möhwald, H. *Langmuir* **1998**, *14*, 2112–2118.
(5) Petrov, J. G.; Brezesinski, G.; Krasteva, N.; Möhwald, H. *Langmuir* **2001**, *17*, 4581.
(6) Gericke, A.; Huenerfuss, H. *Ber. Bunsen-Ges. Phys. Chem.* **1995**, *99*, 641–650.

10.1021/la8009282 CCC: $40.75
Published on Web 07/04/2008

next-nearest-neighbors) yields two peaks with nonzero Q_z maxima, $Q_z^{\mathrm{n}} > 0$ and $Q_z^{\mathrm{d}} > 0$. In both NN and NNN tilted phases, the nondegenerate and degenerate peaks are easily distinguished, because the ratio $Q_z^{\mathrm{n}}/Q_z^{\mathrm{d}}$ can only be 0 or 2. For untilted phases, the integrated peak intensities $I_{xy}^{\mathrm{d}}/I_{xy}^{\mathrm{n}}$ should give a ratio close to 2. The tilt angle can be determined from the formula:

$$\tan\tau = \frac{Q_z^{\mathrm{d}}}{\sqrt{(Q_{xy}^{\mathrm{d}})^2 - (Q_{xy}^{\mathrm{n}}/2)^2}} \text{ for NN tilt with } Q_z^{\mathrm{n}} = 0 \quad (1)$$

$$\tan\tau = \frac{Q_z^{\mathrm{n}}}{Q_{xy}^{\mathrm{n}}} \text{ for NNN tilt with } Q_z^{\mathrm{n}} \neq 0 \quad (2)$$

Rectangular unit cell parameters a_{r} and b_{r} are more appropriate for orthorhombic lattices. For the case of NNN tilted chains discussed later, they are related to the primitive cell parameters by the relationships $a_{\mathrm{r}} = a, b_{\mathrm{r}} = 2b\cos(\gamma - 90°), A_{xy} = a_{\mathrm{r}}b_{\mathrm{r}}/2$. The parameters of the reciprocal lattice normal to the chains, $a_{\mathrm{r}\perp} = a_{\mathrm{r}}$, $b_{\mathrm{r}\perp} = b_{\mathrm{r}}\cos\tau$, $A_0 = A_{xy}\cos\tau$, remove the effect of the tilt and enable comparison of the packing of the chains in tilted and untilted phases.

IRRA Spectra of the Monolayers and Bulk Transmission IR Spectra. IRRA spectra of the FEA monolayers were recorded at 4 cm^{-1} resolution and 200 scans per sample on a Bruker IFS 66 FTIR spectrometer (Karlsruhe, Germany). The principle of the method and its application to Langmuir films at the air−water interfaces are described in ref 7. In our measurements, the incident beam inclined at 62° from the surface normal was p-polarized by a BaF_2 polarizer, and the reflected beam was registered by a MCT detector cooled with liquid nitrogen. A shuttle system moved two compartments of the Langmuir trough with the same liquid level under the laser spot to alternatively measure the reflectivity from the monolayer R_{m} and the neat water surface R_{w} at the same number of scans. The whole setup was sealed in a box maintaining constant water vapor pressure above the film and water surface. This construction practically eliminated the frequency-dependent isotropic contribution of water to the relative reflection−absorption signal $\mathrm{RA} = -\lg(R_{\mathrm{m}}/R_{\mathrm{w}})$ of the monolayer[8] (see also Figures 5 and 6 of this study). The IRRA spectrum was recorded at constant surface pressure of 15 mN/m after we checked that the molecular area did not change with time under such conditions.

The IRRA spectra of the monolayer were compared with the transmission IR spectra of solid FEA in KBr pellet and FEA dilute solution in CCl_4 (1×10^{-3} M, 1 mm KBr cuvette). The bulk spectra were recorded at 2 cm^{-1} resolution and 32 scans per sample on a FTIR spectrometer Bruker IFS 113v. Because no precautions were taken to use a dry KBr pellet, the blank spectrum of the matrix was subtracted to obtain a dry solid FEA spectrum. The transmission IR and the IRRA spectra were normalized by the intensity of the asymmetric CH_2 stretching peak in the corresponding medium. The relative IRRA spectra of the monolayer and the neat water surface are compared without normalization to illustrate the suppression of the isotropic water contribution at the wavenumber ranges of interest.

Results and Discussion

Surface Potentials ΔV and Vertical Components of the Molecular Dipole Moment $\mu_\perp$ of the $RCONHCH_2CF_3$ and $RCOOCH_2CF_3$ Monolayers. Our previous study[3] has shown that the surface potentials at the maximum monolayer density $\Delta V_{\max}$, achieved at the inflection points of the surface pressure/molecular area isotherms π/A, have opposite signs and strongly different values, $\Delta V_{\max}(\mathrm{FEA}) = +1.130$ V, $\Delta V_{\max}(\mathrm{FEE}) = -0.355$ V. The corresponding vertical components of the molecular dipole moment $\mu_{\perp,\max} = A\Delta V_{\max}\varepsilon\varepsilon_0$ also dramatically differ; the values obtained with a relative permittivity of the monolayer $\varepsilon = 7$ are $\mu_{\perp,\max}(\mathrm{FEA}) = +4.06$ D and $\mu_{\perp,\max}(\mathrm{FEE}) = -1.26$ D, respectively. Because the π/A isotherms do not show any plateaus or kinks characterizing specific phase transitions, a direct structural analysis of the $RCONHCH_2CF_3$ and $RCOOCH_2CF_3$ films is necessary to better understand the above $\Delta V_{\max}$ and $\mu_{\perp,\max}$ differences.

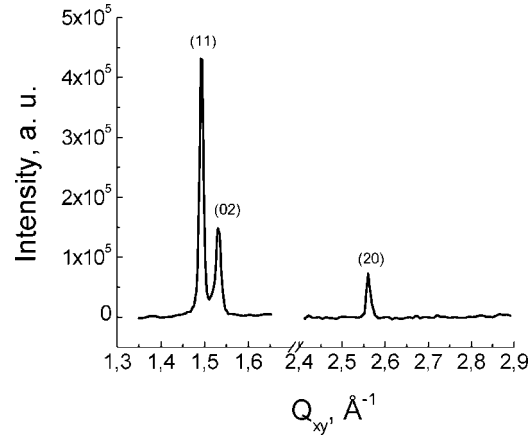

Figure 1. Scattered intensity in the monolayer plane vs the position of the Q_{xy} peaks for the FEA film at 0.3 mN/m and 40.0 Å^2.

Table 1. In-Plane Q_{xy} and Out-of-Plane Q_z Components of the Scattering Vector of the FEA Monolayer[a]

π [mN/m]	Q_{xy} [11] [Å^{-1}]	Q_z [11] [Å^{-1}]	Q_{xy} [02] [Å^{-1}]	Q_z [02] [Å^{-1}]
0.3(40 Å^2)	1.493(0.009)	0.322(0.157)	1.532(0.014)	0.644(0.157)
1.8	1.494(0.009)	0.325(0.158)	1.534(0.011)	0.651(0.158)
4.8	1.495(0.010)	0.329(0.160)	1.535(0.012)	0.658(0.160)
9.9	1.495(0.010)	0.326(0.162)	1.537(0.016)	0.651(0.162)

[a] The fwhm of the peaks is given in parentheses.

Table 2. Primitive Unit Cell Parameters of the FEA Monolayer

π [mN/m]	a [Å^{-1}]	$b = c$ [Å^{-1}]	α [deg]	$\beta = \gamma$ [deg]	τ [deg]	A_{xy} [Å^2]	A_0 [Å^2]
0.3 (40 Å^2)	4.903	4.778	118.3	120.9	22.80	20.11	18.54
1.8	4.901	4.772	118.2	120.9	23.00	20.07	18.48
4.8	4.897	4.770	118.2	120.9	23.20	20.05	18.43
9.9	4.900	4.766	118.1	120.9	22.96	20.03	18.44

GIXD Analysis of the Phase State and Molecular Structure of the $RCONHCH_2CF_3$ Monolayer. Figure 1 shows that the FEA film displays two first order peaks, the degenerate [11] and the nondegenerate [02] one, as well as a second order peak [20]. Table 1 gives the coordinates of the peak maxima and their fwhm at 0.3 mN/m (40 Å^2), 1.8, 4.8, and 9.9 mN/m. The nonzero values of Q_z[11] and Q_z[02] and their ratio $Q_z[02]/Q_z[11] = 2$ define a L_2' phase with an orthorhombic unit cell and NNN tilt of the chains. As expected for such lattice, the nondegenerate [02] peak has higher values $Q_{xy}[02] > Q_{xy}[11]$ and $Q_z[02] > Q_z[11]$.

Table 2 presents the primitive unit cell parameters, and Figure 2 plots the rectangular parameters in the horizontal plane a_{r}, b_{r}, A_{xy}, τ as a function of the surface pressure. The top panel of Figure 2 shows that the short side of the rectangular unit cell a_{r}, corresponding to the distance between the nearest neighbors, does not change under compression to 10 mN/m, whereas the long side b_{r} (the NNN distance) slightly shortens. The area per molecule on the water surface A_{xy} and the tilt angle of the chains from the surface normal τ (bottom panel) change to some extent, but this variation falls in the scatter limits so that we consider the mean values $A_{xy} = 20.07 \pm 0.04$ Å^2 and $\tau = 23.0 \pm 0.2°$ as independent of π.

(7) Mendelsohn, R.; Brauner, J. W.; Gericke, A. *Annu. Rev. Phys. Chem.* **1995**, *46*, 305.
(8) Flach, C. R.; Gericke, A.; Mendelsohn, R. *J. Phys. Chem. B* **1997**, *101*, 58.

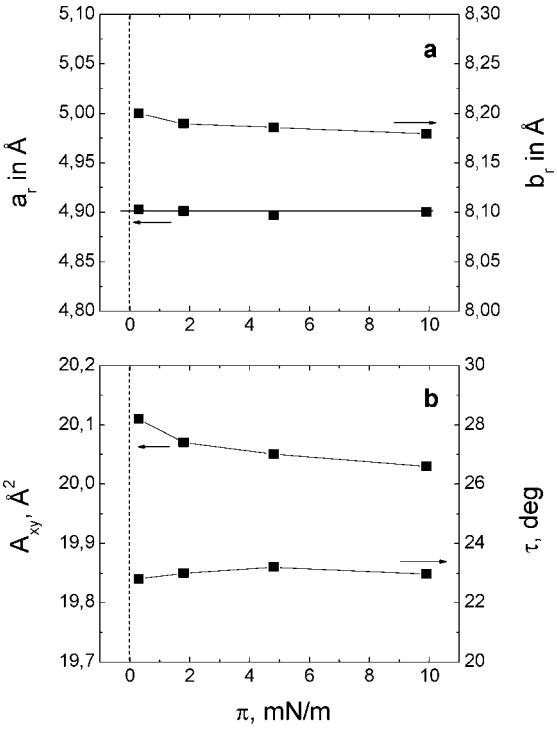

Figure 2. Surface pressure dependencies of the horizontal lattice parameters of the FEA monolayer. Top panel: Rectangular lattice parameters a_r (left) and b_r (right). Bottom panel: Molecular area on the water surface A_{xy} (left), and tilt angle τ of the chains from the surface normal (right).

Comparison of the Micro- and Nanostructure of the $RCONHCH_2CF_3$ and $RCOOCH_2CF_3$ Monolayers. Previous Brewster angle microscopy[5] of the $RCOOCH_2CF_3$ monolayer demonstrated formation of a "Swiss-cheese" morphology after spreading and homogenization of the film below the area of the initial increase of the surface pressure. The parallel GIXD analysis[5] showed that the initial islands and archipelagos have the same CS phase state and unit cell parameters as the homogeneous monolayer with maximum density. These observations imply that the whole increase of the negative surface potential from ΔV of the uncompressed film to ΔV_{max} at maximum film density results from a heterogeneous-to-homogeneous transformation of the microscopic structure, whereas the nanostructure of the FEE monolayer remains unchanged. BAM data for the $RCONHCH_2CF_3$ film (not shown here) display similar morphological transformation in the course of compression. Together with Table 2 and Figure 2 they show that the variation of the microstructure does not influence the nanostructure of the compact parts of the FEA monolayer. Therefore, the whole increase of the positive surface potential from ΔV_{incmp} to ΔV_{max} is caused by homogenization of the FEA film, whose compact parts retain the same L_2' phase and (almost) constant unit cell lattice parameters.

The constant nanostructure of the FEA (left) and FEE (right) monolayers is illustrated in Figure 3, which shows that the positions of the in-plane and out-of-plane diffraction peaks do not change with increasing the surface pressure. The corresponding unit cells and their parameters at 10−12 mN/m are given in the bottom panels, demonstrating that the opposite signs and the dramatic difference of the values of ΔV_{max} correspond to different phase states having tilted versus upright hydrocarbon chains. Tilted phases are usually observed in monolayers with structurally large or/and strongly hydrated polar heads whose chains tilt to closely pack and reduce the free energy in the

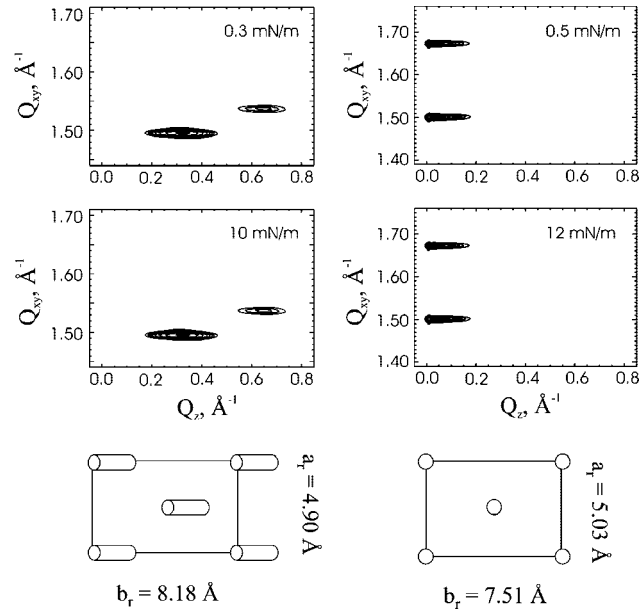

Figure 3. Contour plots of the in-plane Q_{xy} and out-of-plane Q_z scattering vectors of the FEA (left) and FEE (right) films in uncompressed nonhomogeneous (0.3 mN/m, 40.0 Å^2) and compressed homogeneous (10−12 mN/m) monolayers. The corresponding centered rectangular unit cells and their lattice parameters are illustrated in the bottom panels.

film.[9–13] Because the chemical structure of the FEA and FEE heads is similar and their Connolly (water accessible) volumes are close to each other (106.805 Å^3 for $C_2H_5CONHCH_2CF_3$ vs 105.988 Å^3 for $C_2H_5COOCH_2CF_3$), the tilted FEA chains imply a stronger hydration of the amide heads.

Figure 4 puts the reciprocal unit cell parameters of the FEA and FEE monolayers together to compare the packing of the FEA and FEE chains independent of their tilt. Most significant difference exists between $a_{r\perp}$(FEA) = 4.90 Å and $a_{r\perp}$(FEE) = 5.03 Å. The values of $b_{r\perp}$(FEA) form a plateau above 3 mN/m that matches the plateau of the $b_{r\perp}$(FEE) values within the scatter limits. Both $a_{r\perp}$(FEA) and $a_{r\perp}$(FEE) values and both plateau $b_{r\perp}$(FEA) and $b_{r\perp}$(FEE) values do not change under compression. However, the density of the tilted FEA chains is significantly higher than that of the upright FEE chains; the plateau value of A_0(FEA) = 18.4 Å^2, whereas A_0(FEE) = 18.9 Å^2. The denser packing of the same $C_{21}H_{43}$-hydrocarbon chains in the FEA monolayer suggests that the FEA heads cannot be more hydrated than the FEE heads because this would reduce the attraction between the FEA chains and decrease their packing. On the other side, the denser packing of the FEA chains results from the smaller distance between the nearest neighbors (smaller a_r = $a_{r\perp}$ values), whereas the plateau values of $b_{r\perp}$ (NNN distance) of the FEA and FEE films are the same. These relationships imply a stronger anisotropic attraction between the nearest FEA heads. Such features are typical for the H-bonds, which could bind the adjacent FEA molecules via −NH···O═C− bridges as reported for 3D-crystals[14] and Langmuir films[15–18] of other long chain secondary amides.

(9) McIntosh, T. J. *Biophys. J.* **1980**, *29*, 237.
(10) Weideman, G.; Vollhardt, D. *Biophys. J.* **1996**, *70*, 2758.
(11) Weideman, G.; Brezesinski, G.; Vollhardt, D.; Bringezu, F.; de Meijere, K.; Moehwald, H. *J. Phys. Chem.* **1998**, *102*, 148.
(12) Kaganer, V. M.; Osipov, M. A.; Peterson, I. R. *J. Chem. Phys.* **1993**, *98*, 3512–3527.
(13) Kaganer, V. M.; Moehwald, H.; Dutta, P. *Rev. Mod. Phys.* **1999**, *71*, 779.
(14) Rudert, R.; Wu, Y.; Vollhardt, D. *Z. Kristallogr.* **1996**, *211*, 114–116.
(15) Melzer, V.; Weidemann, G.; Vollhardt, D.; Brezesinski, G.; Wagner, R.; Struth, B.; Möhwald, H. *Supramol. Sci.* **1997**, *4*, 391–397.

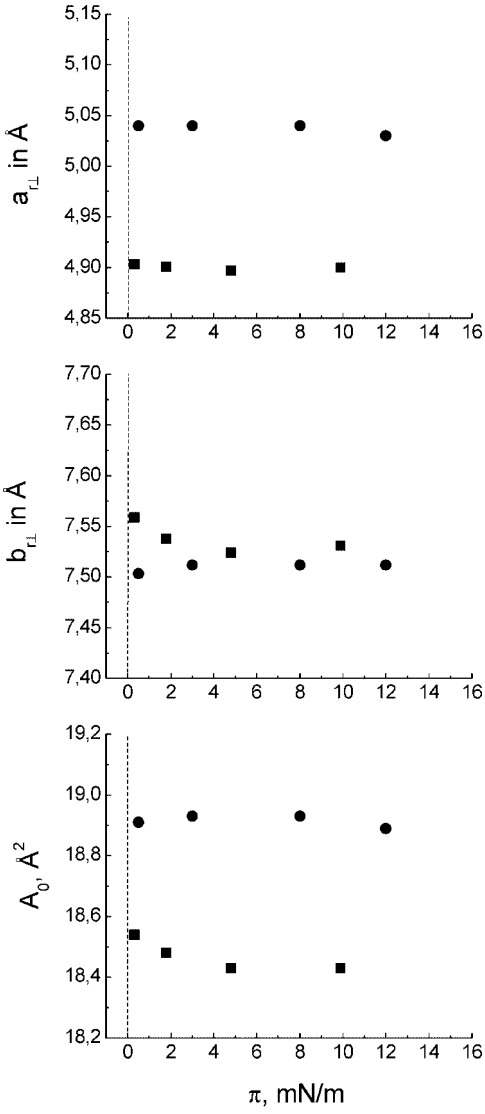

Figure 4. Surface pressure dependence of the parameters $a_{r\perp}$, $b_{r\perp}$, A_0 of the reciprocal lattice, which eliminates the effect of the chain tilt for the FEA (■) and FEE films (●).

IRRAS Analysis of the FEA Monolayer. We applied IRRAS to directly check the existence of −NH···O═C− bonds in the FEA monolayer. It is well-known that such H-bonds shift the peaks of the free stretching vibrations ν(NH) and ν(C═O) to lower wavenumbers and reposition the deformation peak δ(NH) in the opposite direction.[19] For secondary amides as FEA, the ν(NH) peak has different locations for trans and cis conformations of the amide group. The trans isomer, whose N−H and C═O bonds have opposite orientation, exposes the free NH stretching peak at 3460−3400 cm^{-1}; the cis isomer with N−H and C═O bonds pointing in the same direction shows the free NH stretching peak in the range 3440−3420 cm^{-1}. H-bonded trans NH groups exhibit the ν(NH) peak at 3320−3270 cm^{-1}; for H-bonded cis NH groups this peak appears at 3180−3140 cm^{-1}. The trans polar heads are typical for the solid state of open-chain secondary amides RCONHR, where the −NH···O═C− bonds form a lateral

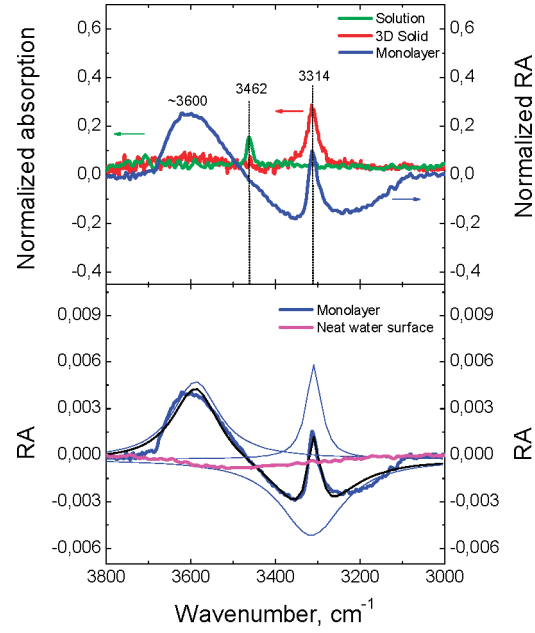

Figure 5. Top panel: Normalized IRRA spectrum of the FEA monolayer (blue), and bulk transmission IR spectra of solid FEA (red) and 1×10^{-3} M FEA solution in CCl_4 (green) in the range 3800−3000 cm^{-1} characteristic for N−H and O−H stretching vibrations. Bottom panel: Lorentz fit (black) and deconvolution (thin lines) of the IRRA spectrum of the FEA monolayer. The blank signal $RA_w = -\lg(R_{w1}/R_{w2})$, comparing the reflectivity R_{w1} and R_{w2} of the neat water surfaces in both trough compartments (magenta), shows almost complete suppression of the isotropic contribution of H_2O and negligible effect on the RA signal of the monolayer.

intermolecular network. Cyclic secondary amides usually have cis polar heads, which form H-bonded dimers.[19]

The RCONHR amides exhibit an intensive ν(C═O) peak (amide I peak), whose position is very sensitive to molecular association. In dilute inert solutions (no −NH···O═C− bonds), this peak appears at 1700−1670 cm^{-1}; the −NH···O═C− bonds in the solid state shift this peak to 1680−1630 cm^{-1}.[19,20] An amide II peak that is specific for the noncyclic secondary amides appears in the range 1540−1510 cm^{-1} for dilute inert solutions, and at ∼1550 cm^{-1} for the solid state.[19] Its nature is complex ν(CN)+δ(NH), but the red shift caused by the breaking of the −NH···O═C− bonds in dilute inert solutions suggests that its deformation component δ(NH) plays the decisive role.[19,20]

Figure 5 (top panel) compares the NH stretching peaks of the transmittance IR spectra of 1×10^{-3} M FEA solution in CCl_4 (green), 3D-solid FEA (red), and the IRRA spectrum of the FEA monolayer (blue). The nonassociated FEA molecules in the CCl_4 solution yield a single ν(NH) peak at 3462 cm^{-1}, typical for the free NH stretching of trans polar heads of secondary amides. The spectrum of the 3D-solid FEA exhibits a single ν(NH) peak at 3314 cm^{-1}, characteristic for H-bonded NH groups of trans heads. The spectrum of the FEA monolayer shows the same single peak at 3314 cm^{-1}, providing evidence that the NH groups of the FEA monolayer are trans oriented and H-bonded. The absence of the free ν(NH) peak at 3462 cm^{-1} in the latter two spectra implies that all NH groups in the 3D and 2D crystals participate in H-bonds.

The complex form of the spectrum of the FEA monolayer suggests an existence of a broad negative band, which overlaps

(16) Melzer, V.; Weidemann, G.; Vollhardt, D.; Brezesinski, G.; Wagner, R.; Struth, B.; Möhwald, H. *J. Phys. Chem. B* **1997**, *101*, 4752–4758.
(17) Melzer, V.; Weidemann, G.; Wagner, R.; Vollhardt, D.; DeWolf, Ch.; Brezesinski, G.; Möhwald, H. *Chem. Eng. Technol.* **1998**, *21*, 44–48.
(18) Melzer, V.; Vollhardt, D.; Weidemann, G.; Brezesinski, G.; Wagner, R.; Möhwald, H. *Phys. Rev. E* **1998**, *57*, 901–906.
(19) Bellamy, L. J. *The Infrared Spectra of Complex Molecules*, 2nd ed.; John Wiley & Sons: New York, 1958; Chapter 12, pp 203−233.
(20) Lee Smith, A. In *Applied Infrared Spectroscopy. Fundamentals, Techniques, and Analytical Problem Solving*; Elving, P. J., Winefordner, J. D., Eds.; John Wiley & Sons: New York/Chichester/Brisbane/Toronto, 1979; Vol. *54*, Appendix 2, p 290.

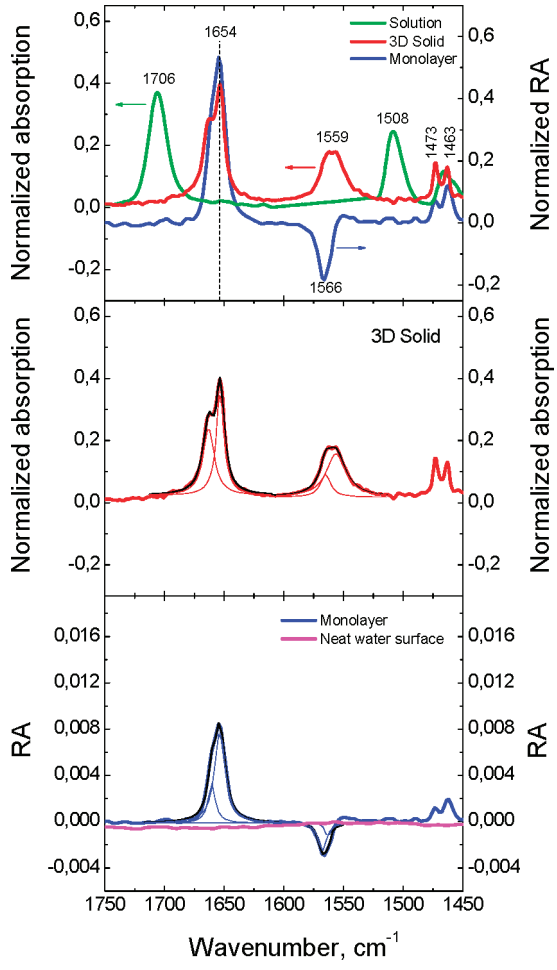

Figure 6. Top panel: Normalized IRRA spectrum of the FEA monolayer (blue), and bulk transmission IR spectra of solid FEA (red) and dilute 1×10^{-3} M FEA solution in CCl_4 (green) in the range of 1750−1450 cm^{-1} characteristic for the ν(C═O) (amide I) and ν (C−N)+δ(N−H) (amide II) peaks. Middle panel: Lorentz fit (black) and deconvolution of the IR spectrum of the 3D-solid FEA (thin lines). Bottom panel: Lorentz fit (black) and deconvolution of the spectrum of the FEA monolayer (thin lines). The negligible blank signal $RA_w = -\lg(R_{w1}/R_{w2})$ (magenta) shows suppression of the isotropic contribution of H_2O.

the ν(NH) peak and shifts its baseline downward. Lorentz fit (the black line in the bottom panel) and deconvolution of the spectrum in three components locate the ν(NH) peak at 3310 cm^{-1} and shift the baseline and the peak to the correct position. Because the blank signal $RA_w = -\lg(R_{w1}/R_{w2})$, comparing the reflectivity R_{w1} and R_{w2} of the neat water surfaces in both trough compartments (magenta), is much smaller than the $RA = -\lg(R_m/R_w)$ signal of the monolayer, we conclude that the deconvoluted positive band centered at 3585 cm^{-1} (fwhm = 133 cm^{-1}) and the negative band centered at 3315 cm^{-1} (fwhm = 183 cm^{-1}) originate from the interfacial water layer beneath the FEA heads. Previous polarization modulated IRRAS investigation of a Langmuir film of cadmium arachidate on water suggested similar interpretation of another negative band at ∼1660 cm^{-1} theoretically assigned to $\delta(OH_2)$ mode of structured water layer under the head-groups.[21–23] Application of the surface specific sum-

(21) Blaudez, D.; Buffeteau, T.; Cornut, J. C.; Desbat, B.; Escafre, N.; Pezolet, M.; Turlet, J. M. *Thin Solid Films* **1994**, *242*, 146.
(22) Blaudez, D.; Turlet, J.-M.; Dufourcq, J.; Bard, D.; Buffeteau, Th.; Desbat, B. *J. Chem. Soc., Faraday Trans.* **1996**, *92*, 525–540.
(23) Blaudez, D.; Buffeteau, Th.; Desbat, B.; Turlet, J.-M. *Curr. Opin. Colloid Interface Sci.* **1999**, *4*, 265.

Table 3. Absorption Maxima of the Deconvoluted Peaks in the Ranges 3800−3000 cm^{-1} and 1750−1500 cm^{-1}

medium	W, cm^{-1}	shift from the solution, cm^{-1}	assignment
CCl_4	3462		ν(trans NH) free
CCl_4	1705.5		ν(C═O) free
CCl_4	1507.5		ν(CN)+δ(NH) free
KBr	3314	−148	ν(trans NH) bonded
KBr	1663.0	−42.5	ν(C═O) bonded
KBr	1653.3	−52.5	ν(C═O) bonded
KBr	1565.1	+57.6	ν(CN)+δ(NH) bonded
KBr	1556.3	+48.8	ν(CN)+δ(NH) bonded
ML	3310	−152.0	ν(trans NH) bonded
ML	1660.5	−45.0	ν(C═O) bonded
ML	1653.6	−51.9	ν(C═O) bonded
ML	1568.3	+60.8	ν(CN)+δ(NH) bonded
ML	1563.0	+55.5	ν(CN)+δ(NH) bonded

frequency vibration spectroscopy at SSP polarization combination (p-polarized IR-input) showed a similar positive band at 3560−3580 cm^{-1} for undissociated hexadecanoic acid monolayer (substrate pH 2.0) that was interpreted as a "signature of a disordered hydrogen-bonded network of the fatty acid−monolayer−water interface".[24] The position of the maximum of the negative IRRAS band at 3315 cm^{-1} and its large fwhm suggest that it probably includes the SFVS broad bands at ∼3200 and ∼3400 cm^{-1} usually assigned to the stretching modes of bonded OH in "ice-like" and "liquid-like" interfacial water structures, respectively.[25]

The top panel of Figure 6 compares the FEA spectra in the same matrices in the range 1750−1450 cm^{-1}. The spectrum in dilute CCl_4 solution (green) shows the amide I peak at 1706 cm^{-1} and the amide II peak at 1508 cm^{-1}, which demonstrate that the C═O and the N−H groups do not participate in H-bonds. The ν(C═O) peak of the 3D-solid FEA (red) has two components both located in the range 1680−1630 cm^{-1} characteristic for H-bonded carbonyls of secondary noncyclic amides.[19] The maximum of the amide I peak of the FEA monolayer (blue) matches the position of the maximum of the same peak in 3D-solid FEA. The absence of the 1705 cm^{-1} peak in both systems shows that all C═O groups in the 3D solid and the monolayer are involved in intermolecular H-bonds. The amide II peak in the 3D-solid FEA at 1559 cm^{-1} also has two components, both blue-shifted from the δ(NH) peak in CCl_4. The asymmetric negative amide II peak of the monolayer at 1566 cm^{-1} is even more shifted from the peak at 1507 cm^{-1} in dilute CCl_4 solution. The positions of these peaks in the spectra of the 3D-solid and the monolayer and the absence of the peak at 1507 cm^{-1} prove that all NH groups in these systems participate in H-bonds. The larger shift of the δ(NH) peak in the FEA film shows that the N−H deformation needs more energy in the monolayer than in the 3D lattice and suggests that the 2D crystal is denser than the 3D one. The split of the CH_2 deformation mode that appears as a single peak at 1466 cm^{-1} in CCl_4, and as a doublet at 1473, 1463 cm^{-1} for the 3D solid and the monolayer, shows that both 3D and 2D lattices have orthorhombic unit cells in accordance with the above GIXD data.

The two components of the amide I and amide II peaks in the bulk IR spectrum of the solid FEA and the asymmetry of these peaks in the IRRA spectrum of the FEA monolayer imply that the NH and O═C groups form two different H-bonds. The Lorentz fit and the number and position of the deconvoluted peaks (see the middle and bottom panels and Table 3) support this conclusion. The amide I peaks in the 3D-solid and monolayer matrices have

(24) Miranda, P. B.; Du, Q.; Shen, Y. R. *Chem. Phys. Lett.* **1998**, *286*, 1.
(25) Shen, Y. R.; Ostroverkhov, V. *Chem. Rev.* **2006**, *106*, 1140–1154.

two components, which are differently red-shifted from the ν(C═O) peak in CCl_4 solution. The corresponding amide II peaks also consists of two components unequally blue-shifted from the deformation peak in CCl_4 solution. The shifts of the amide I and II peaks of the monolayer exceed those of the 3D-solid FEA, indicating a closer packing in the 2D molecular architecture. The blank signal RA_w (magenta) is negligible also in this part of the spectrum, demonstrating that the above analysis of the monolayer is not affected by isotropic water contributions.

Similar complex ν(C═O) peaks were found in the IRRAS spectra of undissociated (pH 2.0) stearic acid monolayers. They show that the uncharged carboxylic heads yield two peaks at 1723 and 1708 cm^{-1} resulting from H-bonds with OH groups of adjacent heads or with hydration water molecules.[26] The origin of the different −NH···O═C− bonds found in this study is so far unclear. One could speculate that the two free electronic pairs of the carbonyl oxygen bind two NH groups, a NH group and a hydration water molecule, or that a H_2O molecule bridges the NH and O═C groups of the next-nearest neighbors along b_r. Ab initio calculations[27] of the H-bonds of trans amide−water and trans amide−trans amide complexes of the secondary *N*-methylacetamide show that their strengths and lengths are similar (ΔH^{298} differ by 0.8 kcal/mol and the lengths by 0.08 Å), so that all above scenarios yielding 2D networks between the FEA heads might be possible.

Structural Difference, Vertical Molecular Dipole Moments, and Surface Dipole Potentials of $RCONHCH_2CF_3$ and $RCOOCH_2CF_3$ Monolayers. The contribution of the hydrocarbon tails (t), hydrophilic heads (h), and hydration water (w) to the vertical molecular dipole moment $\mu_\perp$ and the surface dipole potential ΔV of uncharged condensed monolayers is usually analyzed via the three-capacitor model $\mu_\perp/\varepsilon = \mu_w/\varepsilon_w + \mu_h/\varepsilon_h + \mu_t/\varepsilon_t = \varepsilon_0 A\Delta V$ distinguishing the local dipole moments and permittivities of the above parts of the film.[28] Because ε_w, ε_h, and ε_h are always positive, their possible dependence on the chains tilt and head-groups conformation cannot explain the opposite signs of $\mu_\perp$ and ΔV. Such a difference could exist only if at least one of the μ_w, μ_h, μ_t dipole moments is strongly negative in the $RCOOCH_2CF_3$ monolayer. The all-trans conformation of the FEA and FEE chains, demonstrated by their cross-section values A_0 and the split $\delta(CH_2)$ peak, does not contribute to $\mu_\perp$ and ΔV of both monolayers, because the dipole moments of the methylene groups cancel each other. The vertical components of the terminal $^{\delta-}C-(H^{\delta+})_3$ dipoles of the chains are positive (δ^+ points toward air) independent of the tilt. Therefore, μ_t of the closely packed tilted FEA and upright FEE tails cannot be responsible for the opposite sign of $\mu_\perp$ and ΔV of the FEA and EEE films. The −NH···O═C− dipoles seem to play a secondary role because they exist also in the nonfluorinated EA monolayer, whose vertical molecular dipole moment $\mu_{\perp,max}(EA) = +1.20$ D is much smaller than $\mu_{\perp,max}(FEA) = +4.06$ D, and both values are positive in contrast to the negative value of $\mu_{\perp,max}(FEE)$.[3]

Our present GIXD and IRRAS results prove the formation of a −NH···O═C− network between adjacent trans polar heads of the FEA monolayer as illustrated in Figure 7. The H-bonds shorten the distance a_r between the nearest FEA neighbors as compared to a_r in the FEE film and reduce the area per FEA chain in the reciprocal lattice approaching the densest known packing in $C_{33}H_{68}$ crystals ($A_0 = 18.35$ Å^2).[29] Such packing density implies a downward orientation of the terminal $^{\delta+}C-(F^{\delta-})_3$ dipoles and a large positive value of μ_h(FEA), which seems to be the main source of the 240% positive shift of $\mu_{\perp,max}$(FEA) from the $\mu_{\perp,max}$(EA) value.

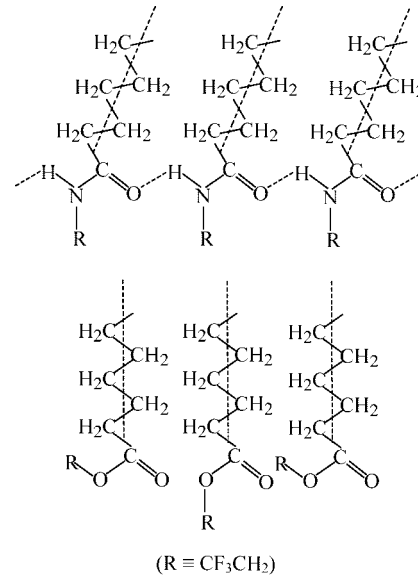

Figure 7. Top panel: Schematic presentation of the −NH···O═C− network, fixing the $^{\delta+}C-(F^{\delta-})_3$ dipoles of the FEA monolayer downward. Bottom panel: Illustration of the statistical upward−downward orientation of $^{\delta+}C-(F^{\delta-})_3$ dipoles in the FEE monolayer. The absence of intermolecular H-bonds between the heads enables the energetically optimal upward orientation of the hydrophobic CH_2CF_3 radicals.

The same downward orientation of the $^{\delta+}C-(F^{\delta-})_3$ dipoles in the $RCOOCH_2CF_3$ monolayer would yield a strong positive μ_h(FEE) value that contrasts with the negative experimental values of $\mu_{\perp,max}(FEE) = -1.26$ D and $\Delta V_{max}(FEE) = -0.355$ V. However, if the majority of the hydrophobic $^{\delta+}C-(F^{\delta-})_3$ dipoles orient upward, satisfying their energetic preference to air, they would make the values of $\mu_{\perp,max}$(FEE) and ΔV_{max}(FEE) negative. Such orientation requires unbounded $-COOCH_2CF_3$ heads enabling free rotation, and enough space for accommodation of the upward oriented CF_3 groups. Early IRRAS studies of monolayers of methyl, ethyl, and *n*-propyl esters of long chain fatty acids have shown[6] that the carbonyl groups of the ethyl and *n*-propyl ester exhibit a single ν(C═O) peak at 1739 cm^{-1} characteristic for unbounded C═O groups, which do not participate in H-bonds and therefore cannot bridge the adjacent polar heads. This result obtained for nonfluorinated ethyl ester heads can be safely transferred to the $C_{21}H_{43}COOCH_2CF_3$ film because the strongly electronegative CF_3 group reduces the oxygen electron density and the ability of the O═C− group to act as H-bond acceptor. On the other side, the nonfluorinated $C_{21}H_{43}COOCH_2CH_3$ monolayer has the same CS phase state and unit cell parameters as the $C_{21}H_{43}COOCH_2CF_3$ film.[5] On the basis of these arguments, we accept that the $C_{21}H_{43}COOCH_2CF_3$ monolayer does not form intermolecular H-bonds in contrast to the $C_{21}H_{43}CONHCH_2CF_3$ film.

A simple molecular modeling minimizing the energy of a monolayer cluster of 36 $C_{21}H_{43}COOCH_2CF_3$ molecules presented in our previous study[3] showed a statistical equilibrium distribution of the conformations of the heads with prevailing upward orientation of the $^{\delta+}C-(F^{\delta-})_3$ dipoles even in closely packed monolayers (Figure 7 bottom). This distribution yields a negative average dipole moment $\mu_{\perp,max}$(FEE) and an average area per molecule $A = 19.3$ Å^2 that is in surprising agreement with the experimental GIXD value of $A_{xy} = 18.9 \pm 0.2$ Å^2. The same statistical orientation of the nonfluorinated $-COOCH_2CH_3$ heads yields positive sign of $\mu_{\perp,max}$(EE), and correct average molecular

(26) Gericke, A.; Huehnerfuss, H. *J. Phys. Chem.* **1993**, *97*, 12899–12908.
(27) Dixon, D. A.; Dobbs, K. D. *J. Phys. Chem.* **1994**, *98*, 13435–13439.
(28) Demchak, R. J.; Fort, T., Jr *J. Colloid Interface Sci.* **1974**, *46*, 191.
(29) Ewen, B.; Strobl, G. R.; Richter, D. *Faraday Discuss.* **1980**, *69*, 19.

area, thus removing the main argument put forward in 1937 by Alexander and Schulman[30] that the steric hindrance in condensed films does not allow upward orientation of the ethyl ester radicals.

The presented IRRAS data are not enough to analyze the contribution of the structured water beneath the heads, which could be different for the $RCONHCH_2CF_3$ and $RCOOCH_2CF_3$ monolayers. We still do not know why Langmuir films of such similar amphiphiles form different L2′ versus CS phases with tilted versus untilted closely packed chains. These questions require a more detailed spectroscopic comparison of the above monolayers and their nonfluorinated analogues, as well as investigation of other similar systems.

Conclusions

Comparison of the molecular structure of $RCONHCH_2CF_3$ and $RCOOCH_2CF_3$ monolayers via in situ X-ray diffraction at grazing incidence (GIXD) shows different L_2' versus CS phases, which do not change under compression. Their closely packed chains are tilted to the next-nearest neighbors in the $RCONHCH_2CF_3$ film but upright in the $RCOOCH_2CF_3$ monolayer. The packing of the chains in the reciprocal lattice perpendicular to them, which excludes the effect of the tilt, shows the same distance $b_{r\perp}$ between the next-nearest neighbors, but significantly closer nearest neighbors in the $RCONHCH_2CF_3$ film, $a_{r\perp}(FEA) = 4.90$ Å versus $a_{r\perp}(FEE) = 5.03$ Å. This difference implies a specific anisotropic attraction between the adjacent amide heads.

(30) Alexander, A. E.; Schulman, J. H. *Proc. R. Soc. London, Ser. A* **1937**, *161*, 115.

Comparison of the IRRA spectrum of the $RCONHCH_2CF_3$ monolayer with transmission IR spectra of the same substance as bulk solid and dilute CCl_4 solution shows a trans conformation of the $-CONHCH_2CF_3$ heads and complete participation in H-bonds. We speculate that the $-NH\cdots O{=}C-$ lateral network formed in this way prevents the energetically optimal orientation of the hydrophobic $-CH_2CF_3$ terminals toward air. The downward orientation of the $^{\delta+}C-(F^{\delta-})_3$ dipoles makes the dipole moment at the monolayer/water boundary and the dipole potential of the film strongly positive. In contrast, the majority of the unrestrained by H-bonds $-COOCH_2CF_3$ heads orient their hydrophobic $^{\delta+}C-(F^{\delta-})_3$ dipoles toward air, yielding a negative average dipole moment at the monolayer/water boundary and a negative surface dipole potential.

The present study does not clarify the contribution of the structured water beneath the head-groups to the surface dipole potential, which could be different for the $RCONHCH_2CF_3$ and $RCOOCH_2CF_3$ monolayers. Different hydration structure could be responsible also for the L_2' versus CS phases, having respectively tilted versus untilted closely packed chains. These aspects will be addressed in a future spectroscopic comparison of the above amphiphiles and their nonfluorinated analogues, as well as of other similar systems.

Acknowledgment. T.D.A. and J.G.P. are grateful to the Alexander von Humboldt Foundation for the research stipends in the framework of the Stability pact special program, which enabled the experiments in this study. We thank Dr. D. Tzankov from the Institute of Organic Chemistry of the Bulgarian Academy of Sciences for the bulk transmission IR spectra.

LA8009282